PHYSICAL REVIEW B **81**, 100502(R) (2010)

Optical spectroscopy of single-crystalline LaFeAsO

Z. G. Chen, R. H. Yuan, T. Dong, and N. L. Wang
Beijing National Laboratory for Condensed Matter Physics, Institute of Physics, Chinese Academy of Sciences, Beijing 100190, China
(Received 2 November 2009; revised manuscript received 10 February 2010; published 2 March 2010)

Millimeter-sized single crystals of LaFeAsO were grown from NaAs flux and the in-plane optical properties were studied over a wide frequency range. A sizable electronic correlation effect was indicated from the analysis of the free-carrier spectral weight. With decreasing temperature from 300 K, we observed a continuous suppression of the spectral weight near 0.6 eV. But a spin-density-wave gap formation at lower energy scale was seen only in the broken-symmetry state. We elaborate that both the itinerancy and local-spin interactions of Fe 3*d* electrons are present for the FeAs-based systems; however, the establishment of the long-range magnetic order at low temperature has a dominantly itinerant origin.

DOI: 10.1103/PhysRevB.81.100502 PACS number(s): 74.70.Xa, 74.25.Gz, 74.25.Jb

The discovery of superconductivity in the ferropnictides[1] has created tremendous interests in the scientific community. While the initial research has mainly concentrated on the compounds with ZrCuSiAs (1111)-type structure, e.g., RFeAsO$_{1-x}$F$_x$ (R=La,Ce,Sm,Pr,Nd, etc.), the focus in the community has been shifted to other structural type compounds, e.g., AFe$_2$As$_2$ (122), Fe(Te,Se) (11), and Na$_x$FeAs (111) systems. This is mainly due to the lack of large-size single-crystal samples in 1111 systems. The crystal growth in 1111 systems has been proven to be difficult. Despite tremendous efforts over the past one year and a half, the single crystals grown by various attempts or methods are limited to small dimensions, typically less than 300 μm.[2,3] As the superconductivity in Fe pnictides was first discovered in a 1111 system[1] and the highest T_c was also achieved in this structural type,[4] the 1111 systems are of special interest. Very recently, Yan *et al.*[5] reported a successful growth of millimeter-sized single crystals of pure and doped LaFeAsO from NaAs flux, which opens the door to explore the physical properties of single-crystal samples of 1111 systems.

Among different physical measurement techniques, optical spectroscopy is powerful in probing the electronic excitations and charge dynamics. It plays a key role in identifying an energy gap and determining the spectral weight and transport lifetime of quasiparticles. Optical studies on 1111 compounds have been done by several groups since the discovery of superconducting LaFeAsO$_{1-x}$F$_x$.[6–11] Except for a work on LaFePO,[11] all measurements were performed on polycrystalline samples. However, LaFePO appears very different from LaFeAsO as no structural and magnetic instabilities were found for it, while the measurements on polycrystalline samples always mix the electronic contributions from the *ab* plane and the *c* axis which could be very different for the quasi-two-dimensional materials, thus leading to ambiguous information. For example, the in-plane plasma frequency is a quantity containing important information about carrier density or many-body effect on the effective mass. As the overall reflectance measured on polycrystalline sample is rather low and drops quickly with increasing frequency, for example, $R(\omega)$ drops to a value of $\sim$0.2 at about 3000 cm^{-1}, it is hard to obtain a reliable value of plasma frequency from those data and, in fact, the values estimated by different groups are rather scattered.[8,9] In this work we report an in-plane optical spectroscopy study on a parent LaFeAsO crystal grown by NaAs flux. We show that the optical spectra of the single-crystal sample are very different from the early measurements on polycrystalline samples, but resemble closely to the in-plane optical response in other FeAs-based parent systems over broad frequencies. The study enables us to identify a strong correlation effect and a partial energy gap formation in the spin-density-wave (SDW) state for LaFeAsO.

The LaFeAsO single crystals used in this work were grown from a procedure similar to that described by Yan *et al.*[5] NaAs, which was found to be an effective solvent for RFeAsO, was prepared first by reacting Na and As chunks at 300 °C in a Al$_2$O$_3$ crucible sealed in quartz tube. LaFeAsO from the mixture of LaAs, 1/3 Fe$_2$O$_3$, and 1/3 Fe was mixed with NaAs flux in a molar ratio of 1:20 and sealed in a Ta tube under 1/2 atmosphere of argon gas. The Ta tube was then sealed in an evacuated quartz tube and heated to 1180 °C at a rate of 60 °C/h. After holding at this temperature for 20 h, it was cooled to 600 °C at 3 °C/h, then quenched to room temperature. Platelike crystals with surface dimensions of $(2-3)\times 3$ could be easily obtained by rinsing flux with water.

Figure 1 shows the in-plane dc resistivity and magnetic susceptibility as functions of temperature. The resistivity was measured by a standard four-probe method. The magnetic susceptibility was measured in a Quantum Design superconducting quantum interference device vibrating-sample magnetometer system under a magnetic field of 1 T with $H\|ab$ plane. The resistivity decreases slightly with decreasing temperature from 300 to 250 K, then increases somewhat with further decreasing temperature. A careful inspection indicates that the slope of the T-dependent resistivity $\rho(T)$ changes near 150 K then shows a cusp near 132 K. $\rho(T)$ drops from 132 to 100 K then increases fast at lower temperature. The two transitions near 150 and 132 K could be seen more clearly if we plot the derivative of resistivity $d\rho(T)/dT$ as a function of T, shown in the inset of Fig. 1. They also manifest in magnetic susceptibility as two weak steps. From the neutron-scattering experiments,[5] it is clear that the two transitions correspond to structural and magnetic transitions. The overall resistivity and magnetic susceptibility are similar to those seen in polycrystalline samples.[6,12] The stronger increase in resistivity at low temperature could be ascribed to certain defects formed in the growth process.

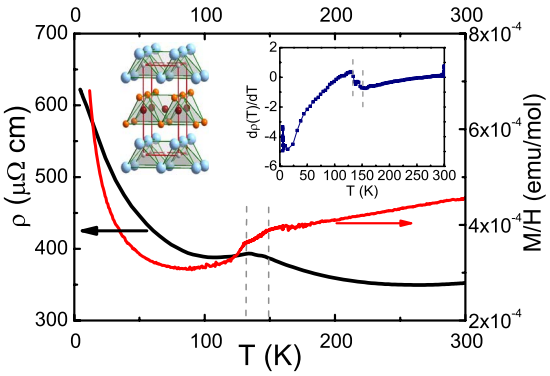

FIG. 1. (Color online) The dc resistivity and magnetic susceptibility vs temperature for LaFeAsO single crystal. Two anomalies could be identified at the dash lines positions. Inset: the derivative of resistivity vs temperature. A crystal structure for LaFeAsO is also drawn.

The optical measurement was done on a Bruker IFS 66v/s spectrometer on a fresh surface of 2×2 mm^2 area in the frequency range from 40 to 25 000 cm^{-1}. An *in situ* gold and aluminum overcoating technique was used to get the reflectance $R(\omega)$. The real part of conductivity $\sigma_1(\omega)$ is obtained by the Kramers-Kronig transformation of $R(\omega)$. Figure 2 shows the room-temperature optical reflectance and conductivity spectra over broad frequencies up to 25 000 cm^{-1}. The overall spectral line shapes are very different from the data measured on polycrystalline samples where the reflectance drops to a value below 0.2 near 3000 cm^{-1},[8,10] but here $R(\omega)$ is still higher than 0.6 near 3000 cm^{-1}. On the other hand, the data on LaFeAsO crystal are very similar to those obtained on AFe_2As_2 (A=Ba, Sr) single crystals.[13–15] The reflectance drops almost linearly with frequency at low-ω region, then merges into the high values of a background contributed mostly from the interband transitions from the mid-infrared to visible regime.

The conductivity spectrum $\sigma_1(\omega)$ displays a Drude-like component at low frequencies. An important quantity that could be extracted from those data is the in-plane plasma frequency ω_p. Within a single-band nearest-neighbor tight-binding model, the kinetic energy of the electrons could be obtained from the summarization of the spectral weight from the free carriers,[11,16] which is proportional to the square of the plasma frequency. The plasma frequency could also be directly obtained from the density-function band-structure calculations.[10,17] Then, the ratio of the experimental kinetic energy and the theoretical kinetic energy from band-structure calculations, which is equal to the ratio of the square of the experimental plasma frequency and the square of band theory plasma frequency, $K_{exp}/K_{band}=\omega^2_{p,exp}/\omega^2_{p,band}$, provides a measure for the renormalization effect from the electron correlations. K_{exp}/K_{band} is close to unity for a simple metal, but is reduced to zero for a strongly correlated Mott insulator. For Fe pnictides, the next-nearest-neighbor interaction, and the multiorbitals to play roles, the above relation should be modified. However, in the absence of a detailed theory, we still use the relation for a rough measure.

From the partial sum rule, the effective carrier density per Fe site below a certain energy ω can be obtained from

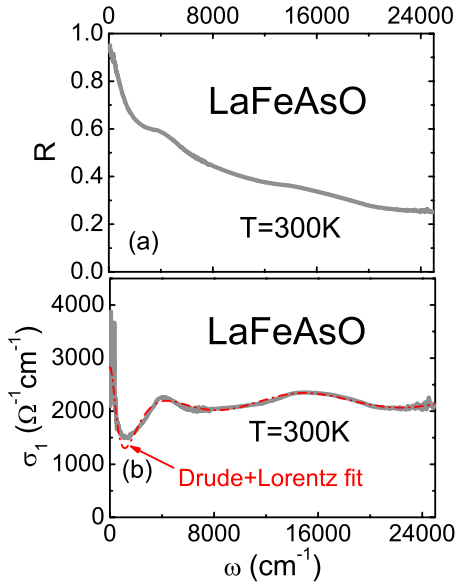

FIG. 2. (Color online) The room-temperature (a) optical reflectance and (b) conductivity for LaFeAsO single crystal over broad frequencies up to 25 000 cm^{-1}. An analysis of the conductivity spectrum by the Drude-Lorentz model is displayed as the dashed curve.

$$\frac{m}{m^*}N_{eff}(\omega)=\frac{2mV_{cell}}{\pi e^2 N}\int_0^{\omega}\sigma_1(\omega')d\omega', \quad (1)$$

where m is the free-electron mass, m^* is the effective or renormalized optical mass, V_{cell} is a unit-cell volume, and N is the number of Fe ions per unit volume. N_{eff} is related to an overall plasma frequency, after choosing a proper high-frequency limit ω_c, via the relationship $\omega_p^2=4\pi e^2N_{eff}(\omega_c)/m^*(V_{cell}/N)=8\int_0^{\omega_c}\sigma_1(\omega')d\omega'$. Choosing $\omega_c\approx1400$ cm^{-1}, a frequency where $\sigma_1(\omega)$ reaches its minimum but below the interband transition, we get the plasma frequency $\omega_p\approx1.01\times10^4$ cm^{-1} for T=300 K.

An alternative way of making quantitative analysis is to fit the conductivity spectrum by a Drude-Lorentz model to isolate the different components of the electronic excitations,

$$\sigma_1(\omega)=\frac{\omega_p^2}{4\pi}\frac{\Gamma_D}{\omega^2+\Gamma_D^2}+\sum\frac{S_j^2}{4\pi}\frac{\Gamma_j\omega^2}{(\omega_j^2-\omega^2)^2+\omega^2\Gamma_j^2}, \quad (2)$$

where ω_p and Γ_D are the plasma frequency and the relaxation rate of conducting electrons, while ω_j, Γ_j, and S_j are the resonance frequency, the damping, and the mode strength of each Lorentz oscillator, respectively. With a Drude component and three Lorentz oscillators centered at 4300, 16 000, and 32 000 cm^{-1}, describing the interband transitions, the experimental data could be reasonably reproduced over a broad frequency range, as seen in Fig. 2(b). The fit yields $\omega_p=1.04\times10^4$ cm^{-1} and $\Gamma_D=640$ cm^{-1} for spectrum at 300 K. We find that the plasma frequency is in a rough agreement with the value obtained by the sum-rule analysis. Note that the plasma frequency for $BaFe_2As_2$ is around 1.3×10^4 cm^{-1} in the nonmagnetic phase.[13] So LaFeAsO has a slightly smaller plasma frequency. The band-structural calcu-

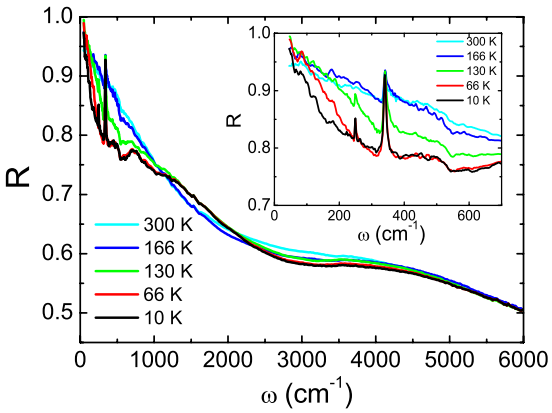

FIG. 3. (Color online) The *ab*-plane reflectance spectra for LaFeAsO below 6000 cm^{-1} at several different temperatures. Inset: the reflectance spectra in the low-frequency region.

lations give the *ab*-plane plasma frequency of 2.1–2.3 eV.[10,17] Then we can estimate that $K_{exp}/K_{band} = \omega^2_{p,exp}/\omega^2_{p,band} \approx 0.30-0.38$. This value is smaller than LaFePO,[11] indicating a stronger reduction in the kinetic energy of the electrons with respect to the band theory. This yields evidence that LaFeAsO is more strongly correlated than LaFePO.

We now turn to the temperature-dependent evolution of the optical spectra. Figure 3 shows the reflectance $R(\omega)$ below 6000 cm^{-1} at several different temperatures. The inset shows the $R(\omega)$ spectra in the range of 0–700 cm^{-1}. The spectra start to show strong temperature dependence below 5000 cm^{-1} (~0.6 eV). Like $BaFe_2As_2$,[13] $R(\omega)$ is suppressed below 5000 cm^{-1} with decreasing temperature, which also leads to the suppression in optical conductivity spectra as shown in Fig. 4. At such high energies, most of the spectral weight should come from the interband transitions; however, the temperature-dependent part must have a different origin. Because this suppression is seen well above the magnetic and structural phase transitions and is present even at room temperature and, furthermore, the energy of 0.6 eV is rather high, it is not directly related to the establishment of the

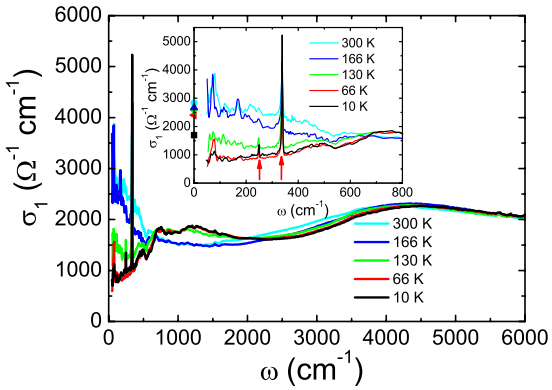

FIG. 4. (Color online) The *ab*-plane conductivity spectra for LaFeAsO below 6000 cm^{-1} at several different temperatures. Inset: an expanded plot of the conductivity spectra in the low-frequency region. The two arrows indicate two phonon peaks. The dc conductivity values at respective temperatures are also shown.

long-range magnetic order. At present the origin of this temperature-dependent structure remains unclear.

More prominent spectral change is seen at lower frequencies when the sample was cooling through the antiferromagnetic SDW transition. The reflectance below 1000 cm^{-1} shows a remarkable suppression, while it is enhanced between 1000 and 2000 cm^{-1}. The spectral change in $R(\omega)$ leads to the redistribution of spectral weight in optical conductivity as seen in Fig. 4. The spectral weight is severely suppressed at low frequencies and the missed spectral weight is transferred to absorption peaks at high energies. This gives optical evidence for the gap formation on the Fermi surfaces below the SDW transition. As we addressed earlier,[13,18] the shape of the spectral weight transfer is governed by the case I coherence factor for a SDW order. Since the reflectance still increases fast toward unity at lower frequencies, residual free carriers or Drude component is still left in the magnetic ordered state. Therefore, the Fermi surfaces are not fully gapped below T_N. All those spectral features are very similar to 122-type AFe_2As_2 (A=Ba,Sr) [13] and 111-type $Na_{1-\delta}FeAs$ single crystals[19] across the SDW transitions, indicating the generic properties of undoped FeAs-based systems.

It should be noted that, although the spectral feature of LaFeAsO resembles to other FeAs-based compounds, $R(\omega)$ does not increase toward unity as fast as in AFe_2As_2 (A=Ba,Sr) below the magnetic or structural transition,[13] and this leads to relatively broad residual Drude component in the SDW state. In the inset of Fig. 4, we show the optical conductivity spectra in the far-infrared region together with the respective dc conductivity values. A good agreement between the dc and optical data at the low-frequency limit could be directly seen at high temperatures. In the low-temperature magnetic state, an upturn feature of the Drude component should be present below our measurement frequencies. However, comparing with the measurement on $BaFe_2As_2$ crystal,[13] the increase in the residual Drude component is less pronounced. The difference is related to the different temperature-dependent behaviors of the dc resistivity. The $BaFe_2As_2$ crystal shows a steep decrease in resistivity below the structural and magnetic transitions, whereas the present LaFeAsO crystal shows only a slight decrease below the magnetic transition; then the resistivity increases rapidly at lower temperature. The peculiar property of the present sample is attributed to the defects formed in the crystal growth.

The origin of the magnetism in the parent compounds of Fe pnictides is one of the focuses in the current research. The above data offer further insight into this issue. The stripe or collinear-type antiferromagnetic order was predicted correctly from the nesting of disconnected electron and hole Fermi surfaces being separated by a (π,π) wave vector at the very beginning,[6] and the importance of electron itinerancy was also addressed by a number of theoretical works.[20–23] Alternatively, the same-type magnetic structure could also be explained by a local-spin Heisenberg exchange model by considering the nearest- and next-nearest-neighbor superexchange interactions.[24–28] So the focus is whether the parent compounds belong to the local or itinerant category of antiferromagnets. Since the compounds are metals, the itinerancy of electrons is apparently present. However, the

strong reduction in the kinetic energy with respect to the density-function band-structural calculations clearly indicates that the material is not a simple metal, but with strong electron correlations. In general, we believe that both the itinerancy and local-spin interactions of Fe 3*d* electrons are present. Nevertheless, the long-range magnetic orders formed at low temperature in FeAs-based compounds are dominantly driven by the nesting tendency. This is because for all undoped FeAs-based systems we observe clear SDW gap openings associated with the transitions. This is expected for a nesting-driven mechanism for the broken-symmetry state, but not the case for the local-spin Heisenberg interactions. On the other hand, for 11-type parent compound FeTe, the local-spin interaction physics seems to dominate the magnetism as no SDW gap formation was observed below the magnetic transition.[29]

Finally, we briefly discuss the infrared phonon lines in the far-infrared region. LaFeAsO crystallizes in the tetragonal $P4/nmm$ structure and according to the factor group analysis, there are six infrared, $3A_{2u}+3E_u$, active modes (along the *c* axis and *ab* plane, respectively).[30] Experimentally we only observe two modes at 248 and 338 cm^{-1} in the *ab*-plane response (see the inset of Fig. 4). The latter mode is particularly strong in intensity. Similar to the case of infrared measurement on the polycrystalline samples,[6] we do not observe any splitting or new phonon lines below the structural or magnetic transition. According to the *ab initio* calculations on LaFeAsO, the splitting of the infrared active phonon modes would be very small and therefore could not be well resolved by the optical measurement.[24] On other hand, the intensities of the two modes show significant temperature dependence. They are strongly enhanced below the structural or magnetic transition. This behavior is similar to the observation in $BaFe_2As_2$ crystal where two infrared active in-plane modes near 94 and 253 cm^{-1} are observed. The two modes are expected for the 122-structure type with $I4/mmm$ space group[31] and the 253 cm^{-1} mode shows a strong intensity enhancement below the structural or magnetic transition. The intensity change was attributed to the charge redistributions at each atom leading to a change in bonding between different atoms.[32] Obviously, the 248 cm^{-1} mode in LaFeAsO is associated with the Fe-As bonds, while the 340 cm^{-1} mode comes from the vibration of oxygen.

To summarize, we studied the *ab*-plane optical properties of LaFeAsO. We show that the optical spectra are very different from the early measurements on polycrystalline samples, but resemble closely to the in-plane optical response in other FeAs-based parent systems over broad frequencies. Our analysis indicates a reduction in kinetic energy of the electrons with respect to the density-function band-structure calculations, thus evidencing a relatively strong correlation effect. A temperature-dependent spectral weight suppression is seen at rather high energy scale, ~0.6 eV, both below and above magnetic and structural transitions. A further partial gap opening at lower energy scales, with a significant spectral weight transfer from the free-carrier region to energies above this gap, is seen only at low temperature in the broken-symmetry state. We elaborate that both the itinerancy and local-spin interactions of Fe 3*d* electrons are present in Fe-based systems, but they have different dominant contributions to the magnetic instabilities for different systems. The long-range magnetic orders formed at low temperature in FeAs-based compounds are dominantly driven by the nesting tendency of disconnected Fermi surfaces.

We thank S. K. Su and Y. R. Zhou for their help in magnetization measurement. This work was supported by the National Science Foundation of China, the Knowledge Innovation Project of the Chinese Academy of Sciences, and the 973 project of the Ministry of Science and Technology of China.

[1] Y. Kamihara *et al.*, J. Am. Chem. Soc. **130**, 3296 (2008).
[2] N. D. Zhigadlo *et al.*, J. Phys.: Condens. Matter **20**, 342202 (2008).
[3] H.-S. Lee *et al.*, Supercond. Sci. Technol. **22**, 075023 (2009).
[4] Z.-A. Ren *et al.*, Chin. Phys. Lett. **25**, 2215 (2008).
[5] J. Yan *et al.*, Appl. Phys. Lett. **95**, 222504 (2009).
[6] J. Dong *et al.*, EPL **83**, 27006 (2008).
[7] A. Dubroka *et al.*, Phys. Rev. Lett. **101**, 097011 (2008).
[8] S.-L. Drechsler *et al.*, Phys. Rev. Lett. **101**, 257004 (2008).
[9] A. V. Boris *et al.*, Phys. Rev. Lett. **102**, 027001 (2009).
[10] S. Drechsler *et al.*, arXiv:0904.0827 (unpublished).
[11] M. M. Qazilbash *et al.*, Nat. Phys. **5**, 647 (2009).
[12] Guang-Ming Zhang *et al.*, EPL **86**, 37006 (2009).
[13] W. Z. Hu *et al.*, Phys. Rev. Lett. **101**, 257005 (2008).
[14] D. Wu *et al.*, Phys. Rev. B **79**, 155103 (2009).
[15] S. Moon *et al.*, arXiv:0909.3352 (unpublished).
[16] D. Baeriswyl *et al.*, Phys. Rev. B **35**, 8391 (1987).
[17] L. Boeri *et al.*, Phys. Rev. Lett. **101**, 026403 (2008).
[18] W. Z. Hu *et al.*, Physica C **469**, 545 (2009).
[19] W. Z. Hu *et al.*, Phys. Rev. B **80**, 100507(R) (2009).
[20] I. I. Mazin *et al.*, Phys. Rev. Lett. **101**, 057003 (2008).
[21] Ying Ran *et al.*, Phys. Rev. B **79**, 014505 (2009).
[22] V. Cvetkovic and Z. Tesanovic, EPL **85**, 37002 (2009).
[23] D. J. Singh, Physica C **469**, 418 (2009), and references therein.
[24] T. Yildirim, Phys. Rev. Lett. **101**, 057010 (2008).
[25] Q. Si and E. Abrahams, Phys. Rev. Lett. **101**, 076401 (2008).
[26] F. J. Ma *et al.*, Phys. Rev. B **78**, 224517 (2008).
[27] C. Fang *et al.*, Phys. Rev. B **77**, 224509 (2008); C. Xu *et al.*, *ibid.* **78**, 020501(R) (2008).
[28] J. Wu *et al.*, Phys. Rev. Lett. **101**, 126401 (2008).
[29] G. F. Chen *et al.*, Phys. Rev. B **79**, 140509(R) (2009).
[30] V. G. Hadjiev *et al.*, Phys. Rev. B **77**, 220505(R) (2008).
[31] A. P. Litvinchuk *et al.*, Phys. Rev. B **78**, 060503(R) (2008).
[32] A. Akrap *et al.*, Phys. Rev. B **80**, 180502(R) (2009).